Experimental study of small ensembles of atoms in a microwave cavity

Barbara J. Hughey,* Thomas R. Gentile,† and Daniel Kleppner
Research Laboratory of Electronics, Department of Physics, Massachusetts Institute of Technology, Cambridge, Massachusetts 02139

Theodore W. Ducas
Wellesley College, Wellesley, Massachusetts 02181
(Received 17 January 1990)

We report results of an experimental study of the evolution of small ensembles of atoms in a microwave cavity. The experiment employs an atomic beam of calcium Rydberg atoms and a split superconducting cavity operating at 35 GHz. At the ambient temperature of 2 K, the mean blackbody photon number is 0.8. Selective field ionization allows us to monitor simultaneously the populations of the initial and final states. The time evolution of the atomic system is probed by "Stark switching," i.e., shifting the atomic resonance away from the cavity resonance by applying an electric field. The collective oscillations of energy between ensembles of atoms and a cavity with $Q > 10^7$ are studied for one to several hundred atoms. The results agree well with theory for ≈ 50 or more atoms, but some discrepancies are observed for smaller numbers of atoms. Possible experimental sources of these discrepancies are discussed.

I. INTRODUCTION

The study of small systems of atoms interacting with cavities has evolved into an identifiable subfield of atomic physics: cavity QED.[1] In this paper we describe a study of the exchange of energy between ensembles of 1–500 atoms and the radiation field in a high-Q cavity. An experimental study of collective atom-cavity oscillations for very large numbers of atoms ($\gtrsim 20\,000$) in a low-Q open confocal cavity has been performed by Kaluzny *et al.*[2] Some related work in cavity QED includes experiments on the inhibition[3,4] and enhancement[5] of spontaneous emission in low-Q cavities. Investigations of atoms interacting with high-Q cavities led to the development of the one-atom maser[6,7] and the two-photon maser.[8] The theory for small systems of atoms in cavities has been developed by a number of authors.[9–12]

We present an experimental study of the dynamics of small ensembles of Rydberg atoms in a high-Q cavity at cryogenic temperatures. Singlet states of calcium, which lack both fine and hyperfine structure, provide an excellent approximation to a two-level atomic system. We use pulsed dye lasers to prepare an atomic beam of calcium Rydberg atoms inside a superconducting cavity. Selective field ionization allows the initial and final state populations to be monitored simultaneously. The cavity mode employed provides a constant radiation field amplitude along the direction of atomic beam propagation so that atoms with different velocities experience the same interaction with the cavity field. The time evolution of the system is probed by "Stark switching," i.e., shifting the atomic resonance away from the cavity resonance by applying an electric field, thereby inhibiting the transition and "freezing" the atomic population.[2] This is accomplished in a superconducting cavity that was split into electrically isolated halves. The Stark switching technique permits the atom-cavity oscillations to be observed with good time resolution for several cycles. In contrast to experiments which depend on velocity selection of an atomic beam to provide time resolution, our method permits observation of the system for arbitrarily short times.

Section II presents a brief review of the theory for ensembles of atoms evolving in a cavity. The apparatus is described in Sec. III. Data on the exchange of energy between the atoms and the cavity are presented in Sec IV. For systems of 50 to 500 atoms, the observations are found to agree well with theory. Although the Q was sufficiently high to allow single atom oscillations, the data for small numbers of atoms in the cavity are more damped than theory predicts. Some explanations for this discrepancy are discussed in Sec. V. Section VI presents conclusions from our research.

II. THEORETICAL BACKGROUND

A. Dynamics of a single atom in a cavity

The behavior of a single two-level atom interacting with a single mode of the radiation field was first discussed by Jaynes and Cummings.[13] An excited two-level atom in a resonant lossless cavity at 0 K will spontaneously exchange energy with the cavity at a frequency ω_a given by[9]

$$\omega_a = \frac{d}{\hbar}\left(\frac{2\hbar\omega_0}{\epsilon_0 V_{\text{eff}}}\right)^{1/2} . \tag{1}$$

V_{eff} is the mode-dependent effective volume of the cavity, ω_0 is the transition frequency, and d is the dipole matrix element between the levels of the atomic system. If the cavity has losses, the system behaves similarly to a pair of coupled classical oscillators undergoing damped harmon-

ic motion. For $\omega/2Q > \omega_a$, where ω is the frequency and Q is the quality factor of the cavity, the system is overdamped and the excited state population decays at a rate proportional to Q. In this paper, however, we are interested only in the underdamped regime, where $\omega/2Q < \omega_a$.

For an underdamped system with the cavity at temperature T and resonant with the atomic transition, the probability $P_e(t)$ that an initially excited atom will be in the excited state at time t is approximately[9]

$$P_e(t)=\frac{\beta}{1+\beta}+\frac{1-\beta}{2(1+\beta)}\exp[-\gamma(1+\beta)t] + \frac{1-\beta}{2}\sum_{n=0}^{\infty}\beta^n\exp(-\gamma t)\cos(\omega_a\sqrt{n+1}\,t)\ , \quad (2)$$

where $\beta=\exp(-\hbar\omega/kT)$ and $\gamma=\omega/2Q$. Because the oscillation frequency for a cavity with an initial photon occupation number of n is $\omega_a\sqrt{n+1}$, the distribution of the number of blackbody photons in the cavity causes $P_e(t)$ to be a superposition of oscillations with incommensurate frequencies. As the temperature increases, interference between these frequencies washes out the oscillations increasingly rapidly.

B. Dynamics of an ensemble of atoms in a cavity

1. Density-matrix approach

The treatment in this section follows Haroche's analysis of ensembles of two-level atoms in a high-Q cavity.[10,11] An ensemble of atoms that is excited in a region of uniform cavity field amplitude must be treated as a system of indistinguishable particles. The states of such a collective N-atom system are the Dicke states,[14] which are equivalent to states of angular momentum $J=N/2$. The Dicke states, which are symmetric under atom exchange, can be labeled $|J,M\rangle$, where $-J\le M\le J$. The number of atoms in the upper state is $J+M$, which ranges from 0 to N. Note that the atomic system remains in a Dicke state only as long as the atoms experience identical conditions. For an atomic beam experiment, this requires that the electric field amplitude along the direction of motion be constant and that no atoms leave the cavity during the interaction time. Otherwise, atoms with different velocities would experience different fields and become, in principle, distinguishable.

The total atom-field Hamiltonian $H_{\rm tot}$ in the rotating-wave approximation is[10]

$$H_{\rm tot}=H_A+H_F+H_{AF} =\hbar\omega_0 D^0+\hbar\omega(a^\dagger a+\tfrac{1}{2})+\tfrac{1}{2}\hbar\omega_a(aD^+ +a^\dagger D^-)\ , \quad (3)$$

where H_A and H_F are the atomic and field Hamiltonians, respectively, and H_{AF} describes the atom-field interaction. a and $a^\dagger$ are the conventional destruction and creation operators for the electromagnetic field. D^+ and D^- are collective atomic raising and lowering operators, respectively, that act on the Dicke states like standard angular momentum raising and lowering operators. D^0 acts on the Dicke states like the z component of the angular momentum operator.

The evolution of the system can be described by the density-matrix equation[10]

$$\frac{d\rho_{A+F}}{dt}=\frac{1}{i\hbar}[H_{\rm tot},\rho_{A+F}]+\Lambda_F\rho_{A+F}\ . \quad (4)$$

The last term in Eq. (4), which accounts for dissipation, is given by

$$\Lambda_F\rho_{A+F}=\frac{-\omega}{2Q(T)}[a^\dagger a,\rho_{A+F}]_+ +\frac{\omega}{Q(T)}a\rho_{A+F}a^\dagger - \frac{\omega}{2Q(T)}\beta[aa^\dagger,\rho_{A+F}]_+ +\frac{\omega}{Q(T)}\beta a^\dagger\rho_{A+F}a\ , \quad (5)$$

where $Q(T)\equiv Q(1-\beta)$ and $[a,b]_+\equiv ab+ba$.

The probability that a member of the system is excited at time t is related to the expectation value of D^0 by

$$P_e(t,N)=\frac{1}{N}\langle D^0\rangle+\tfrac{1}{2}\ . \quad (6)$$

For small numbers of atoms ($N\lesssim 50$) the density-matrix equations expanded in the Dicke state basis can be solved numerically on a small laboratory computer.[15] However, computations become increasingly lengthy as the number of atoms increases. For large numbers, the Bloch vector model provides a more practical approach.

2. Bloch vector model

The Bloch vector model is useful for describing a system composed of a large number of identical atoms.[10,11,16] The time derivatives of the quantum-mechanical operators D^0, D^+, and $a^\dagger$ are found in the Heisenberg picture. The atomic operators are related to the components (η,ρ) of the Bloch vector, a classical angular momentum vector with length $J=N/2$. $D^0\to\eta\equiv\frac{1}{2}N\cos\theta$ and $D^+\to\rho\equiv\frac{1}{2}N(\sin\theta)e^{i\phi}$, where θ and ϕ are the standard angles in spherical coordinates. The field operator $a^\dagger$ is identified with $\mathcal{E}$, a classical electric field in the cavity.[11]

The evolution of the classical quantities η, ρ, and $\mathcal{E}$ is described by[15]

$$\frac{d\eta}{dt}=\frac{-i\omega_a}{2}(\mathcal{E}^*\rho-\mathcal{E}\rho^*)\ , \quad (7a)$$

$$\frac{d\rho}{dt}=-i\omega_a\mathcal{E}\eta\ , \quad (7b)$$

$$\frac{d\mathcal{E}}{dt}=i\delta\mathcal{E}-\gamma\mathcal{E}+\frac{i\omega_a}{2}\rho+\tilde{F}^\dagger(t)\ , \quad (7c)$$

where $\delta\equiv\omega-\omega_0$. Equation (7c) includes a damping term and a random force $\tilde{F}^\dagger(t)$ that account for the coupling of the radiation mode to the thermal reservoir of the cavity walls.

Solving Eqs. (7) is time-consuming because of the random force $\tilde{F}^\dagger(t)$. However, it can be shown[11] that the problem can be simplified by assuming that $\tilde{F}^\dagger(t)=0$ and $\mathcal{E}(t=0)=0$, provided that $\theta(t=0)$ is randomly distributed with a probability distribution

$$P(\theta(0))=\frac{2\theta(0)}{\theta_0^2}\exp\{-[\theta(0)/\theta_0]^2\}\ , \tag{8}$$

where

$$\theta_0=2\left[\frac{\bar{n}+1}{N}\right]^{1/2} \tag{9}$$

is the "average" tipping angle of the Bloch vector in the presence of a thermal distribution of photons with mean number $\bar{n}$. The initial conditions are thus

$$\eta(0)=\tfrac{1}{2}N\cos[\theta(0)]\ , \tag{10a}$$

$$\rho(0)=\tfrac{1}{2}N\sin[\theta(0)]e^{i\phi(0)}\ , \tag{10b}$$

$$\mathcal{E}(0)=0\ . \tag{10c}$$

Because our experiments only measure η, they are not sensitive to ϕ. Therefore $\phi(0)$ can be chosen to be zero. Equations (7) can be readily solved for various values of $\theta(0)$. The probability of excitation at time t is then given by

$$P_e(t,N)=\frac{1}{N}\langle\eta(t,N,\theta(0))\rangle_{\theta(0)}+\tfrac{1}{2}\ , \tag{11}$$

where the average over $\theta(0)$ is carried out using Eq. (8).

Figure 1 compares values of $P_e(t,N=50)$ calculated using the density-matrix method [Eq. (6)] and the Bloch vector method [Eq. (11)]. The Bloch method provides a reasonably accurate solution, though some discrepancy is evident. As N is decreased, however, the Bloch solution becomes progressively less reliable.

3. *"Collapse frequency" $\nu_{\rm col}$*

There is no general way to parametrize the behavior of the atom-cavity system, but for underdamped motion one feature is particularly easy to observe experimentally: this is the time $\tau_{\rm min}$ at which $P_e(t,N)$ achieves its first minimum. We define the "collapse frequency" $\nu_{\rm col}$ by

$$\nu_{\rm col}\equiv(2\tau_{\rm min})^{-1}\ . \tag{12}$$

Although $P_e(t,N)$ is a complicated function of the system parameters, Haroche[10] has pointed out that the variation of $\nu_{\rm col}$ with the number of atoms N can be accurately parametrized by

$$\nu_{\rm col}(N)=\frac{a\sqrt{N}}{b+\ln N}\ , \tag{13}$$

where a and b are adjustable parameters that depend on ω_a, γ, and β. The accuracy of this expression is illustrated by Fig. 2 which displays values of $\nu_{\rm col}$ obtained from the exact solution [Eq. (6)] for $N\leq 50$ and from the Bloch method [Eq. (11)] for $N\geq 200$, along with the best fit of Eq. (13) to the calculations.

C. Effects of fluctuations in N

Because $P_e(t,N)$ is sensitive to N, comparing theory and experiment requires that the effect of fluctuations in the number of excited atoms be considered. Fluctuations arise from normal statistical variations and also from pulse to pulse variations in the frequency and power of our pulsed laser system. The number of atoms N_d detected following each laser pulse is less than N, the number of atoms excited in the cavity, because of detector inefficiency and finite radiative lifetime. Denoting the total detection efficiency by ϵ_d gives $N_d=\epsilon_d N$. The standard deviation in N_d due to statistical fluctuations is

$$\sigma_{\rm stat}=(\bar{N}_d)^{1/2}\ , \tag{14}$$

where $\bar{N}_d$ is the mean number of atoms detected. The standard deviation in N_d due to pulse-to-pulse variations in the lasers is proportional to $\bar{N}_d$:

$$\sigma_{\rm laser}=f_l\bar{N}_d\ . \tag{15}$$

The source of these fluctuations appears to be associated with the laser that drives the final step. (The first two steps in the excitation scheme are strongly saturated in order to reduce f_l.) We assume that the two sources of fluctuations are independent. Consequently, the total

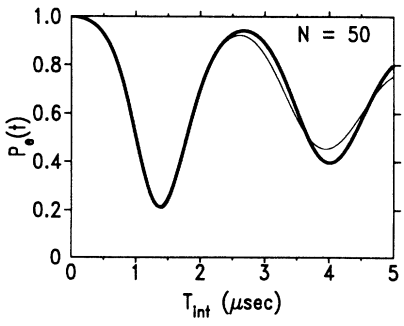

FIG. 1. Comparison of calculations by the exact method (thick line) and the Bloch method (thin line) for 50 atoms in the cavity with $Q=1.2\times10^7$ and $T=2.17$ K. The horizontal axis is the atom-cavity interaction time $T_{\rm int}$ and the vertical axis is the probability that the atom is in the upper state, $P_e(t)$.

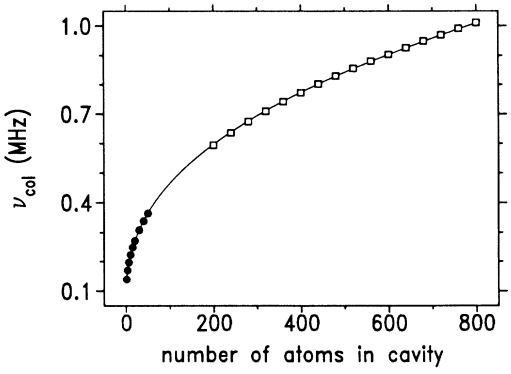

FIG. 2. Dependence of the "collapse" frequency $\nu_{\rm col}$ on number of atoms N for $Q=1.2\times10^7$ and $T=2.17$ K. The closed circles are obtained from the exact method and the open squares from the Bloch method, as discussed in the text. The solid curve is a fit of the calculations to Eq. (13), which yields $a=0.3187$ MHz and $b=2.245$.

standard deviation in N_d is

$$\sigma_{N_d}=(\sigma_{\text{stat}}^2+\sigma_{\text{laser}}^2)^{1/2}$$
$$=[\bar{N}_d+(f_l\bar{N}_d)^2]^{1/2} . \quad (16)$$

The coefficient for laser fluctuations f_l is found by determining the standard deviation σ_{N_d} as a function of $\bar{N}_d$ by measuring N_d for 200–500 laser pulses for each value of $\bar{N}_d$. Figure 3 shows measured values of σ_{N_d} obtained by this procedure and a fit of this data to Eq. (16) yielding f_l. f_l varied from day to day between 0.06 and 0.26. Typically, $f_l=0.14$.

Because f_l is a property of the lasers only, not the size of the sample, σ_N is expected to be identical in form to σ_{N_d} [Eq. (16)]. The measured distribution of N_d is approximately Gaussian, and so we take the distribution in the number of initially excited atoms N to be given by

$$G(N)=\frac{1}{\sqrt{2\pi}\sigma_N}\exp\left[-\frac{1}{2}\left[\frac{N-\bar{N}}{\sigma_N}\right]^2\right] , \quad (17)$$

where $\sigma_N=[\bar{N}+(f_l\bar{N})^2]^{1/2}$.

The time evolution of the system when the mean number of initially excited atoms is $\bar{N}$ is given by

$$\bar{P}_e(t,\bar{N})=\sum_N G(N)P_e(t,N) . \quad (18)$$

The Gaussian distribution [Eq. (17)] is valid only for large values of $\bar{N}$. However, for values of $\bar{N}$ as small as 7, which is the lower limit of our experimental data (excluding single atom experiments for which no averaging is required), the use of a Poissonian instead of a Gaussian distribution has a negligible effect on the calculated value of $\bar{P}_e(t,\bar{N})$.

The most conspicuous effect of the fluctuations is to wash out the oscillations after several periods. This is illustrated in Fig. 4, where $P_e(t,N=300)$ is compared with $\bar{P}_e(t,\bar{N}=300)$, assuming $f_l=0.14$. For small values of $\bar{N}$, the fluctuations wash out the oscillations in a similar manner. In addition, for values of $\bar{N}$ close to 1, the fluctuations can noticeably increase ν_{col}.

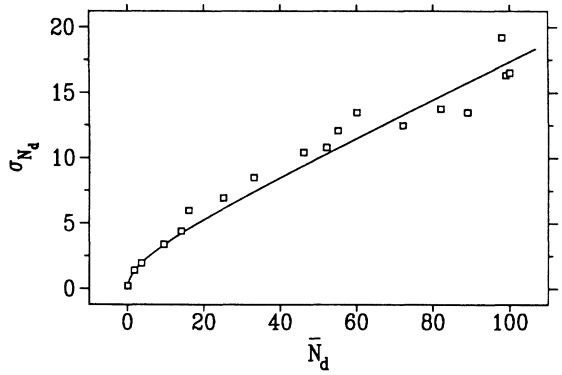

FIG. 3. Measured standard deviation σ_{N_d} vs mean number of detected atoms $\bar{N}_d$. The solid curve is a fit of the data to Eq. (16) which yields $f_l=0.142(6)$. (The number in parentheses denotes the uncertainty in the last digit.)

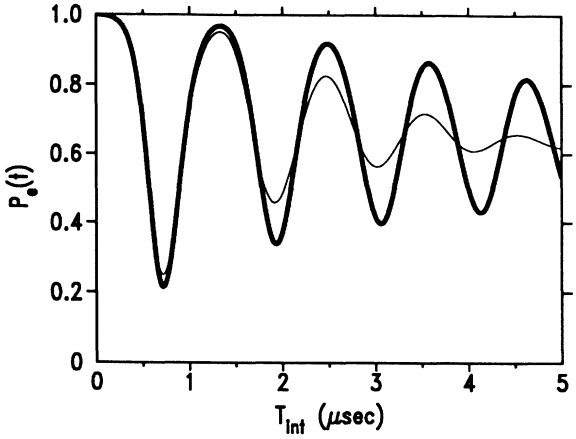

FIG. 4. Calculated evolution of the system with exactly 300 atoms in the cavity (thick line) compared to the evolution with an average of 300 atoms in the cavity (thin line) obtained from Eq. (18) with $f_l=0.14$. T_{int} is the atom-cavity interaction time and $P_e(t)$ is the probability that the atom is in the upper state.

III. EXPERIMENT

The apparatus is similar to that used in our studies of one- and two-photon Rabi oscillations[17] and microwave spectroscopy of calcium Rydberg states.[18] A diagram is shown in Fig. 5. The major change is that the waveguide structure used for driving microwave transitions has been replaced by a microwave cavity. The calcium atomic beam is prepared in the $46p$ state (abbreviation for the $4s46p\ ^1P_1$ state) inside the cavity using a three-step pulsed dye laser system. The final laser beam is polarized along the cavity electric field so that the $46p\,(m=0)$ state is excited relative to this quantization axis. The two states involved in the atom-cavity oscillations are thus the $46p\,(m=0)$ (upper state) and $46s$ (lower state). The frequency of the $46p\rightarrow 46s$ transition in calcium in 35.332 GHz; the atom-cavity coupling frequency $\omega_a/2\pi$ calculated for this transition and our cavity dimensions is 105 kHz. Observing underdamped behavior for a single atom in the cavity requires $Q>2\times10^5$. To avoid washing out the oscillations from the effects of blackbody radiation (Sec. II A), the one-atom experiments require temperatures $\lesssim 2$ K, for which $\bar{n}\lesssim 0.8$.

A 0.38-mm-diam hole in the collimating plate limits the atomic beam diameter inside the cavity to $\lesssim 0.51$ mm. The atoms are excited inside the cavity, 2 mm past the front end cap [Fig. 5(b)]. The mean transit time to the cavity exit is 18 μsec, which corresponds to two cycles of the single-atom–cavity oscillation. After the atoms exit the cavity, they enter the detector region where selective field ionization is used to detect and differentiate the two states. We measure $\bar{P}_e(t,\bar{N})$ for each value of $\bar{N}_d$ by scanning the time t at which a 200-mV pulse is applied between the cavity halves. In this way, we count the number of atoms detected in the $46p$ and $46s$ states as a function of the atom-cavity interaction time. Sample data are shown in Fig. 7. The apparatus is discussed in more detail in Refs. 15, 17, and 19.

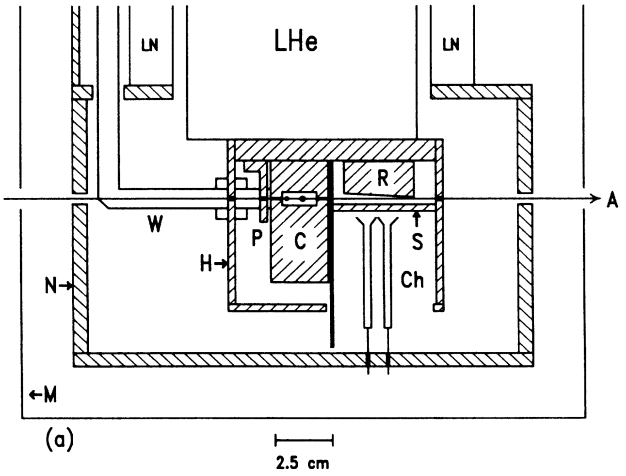

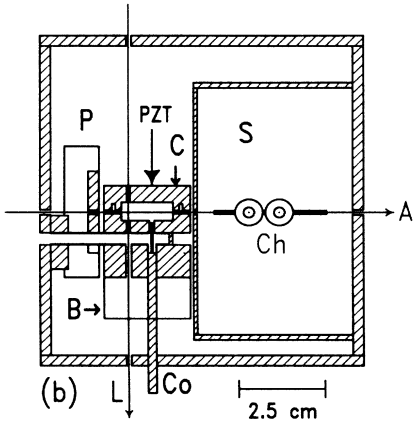

FIG. 5. Diagrams of the apparatus. (a) Side view. (b) Bottom view. *A*, atomic beam; *H*, liquid-helium (LHe) temperature shield; *N*, liquid-nitrogen (LN) temperature shield; *M*, single layer μ-metal shield; *P*, collimating plate; *C*, cavity; *R*, ramped plate; *S*, slotted plate; Ch, channel electron multipliers; *W*, waveguide; *L*, laser beams; *B*, waveguide holder; Co, coupler. The tuning mechanism is not shown for clarity. The location of the PZT is shown schematically.

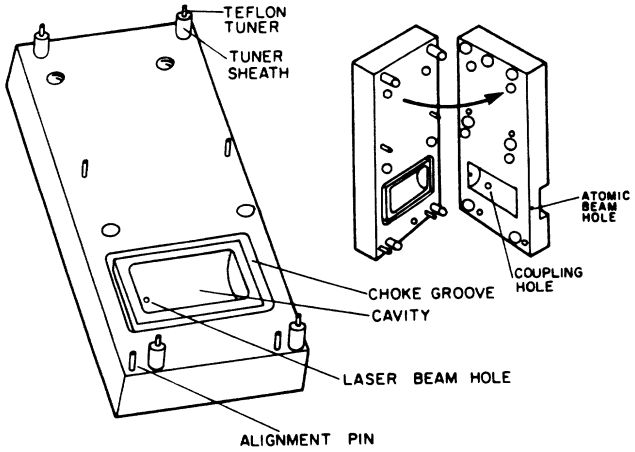

FIG. 6. Drawing of the cavity. The cavity cylinder is 6.5 mm diameter and 15.2 mm long. Each half is constructed from a $7.6\times25.4\times51.6$-mm^3 block of copper. The "movable" half contains the choke groove, and the "fixed" half contains the coupling and atomic beam holes. Also shown are the $\frac{1}{16}$-in.-diam Teflon rods and the $\frac{1}{16}$-in.-diam sapphire alignment pins.

A. Cavity

The cavity is operated in the cylindrical TM_{010} mode. This mode was chosen because the electric field amplitude is constant along the direction of atomic beam propagation, and because the cavity can be split in half lengthwise without seriously disturbing the mode geometry. This allows us to control the atom-cavity interaction time by applying a small voltage between the halves, thereby Stark shifting the atomic transition frequency away from the cavity resonance and "freezing" the atomic population at the moment at which the voltage pulse is applied.

Although splitting the cavity in half should not force currents to cross the gap between the halves, we found initially that a small leakage of power limited the cavity Q to $\leq 2\times10^5$. We achieved $Q>10^7$ in niobium and lead-plated copper cavities by adding a choke groove to trap this microwave power.[20] The split cavity design also allows us to tune the cavity over a large range without significantly degrading the Q, which allows convenient access of the atomic transition frequency. Tuning is accomplished by varying the size of the gap between the halves. Figure 6 shows a drawing of the cavity. Its dimensions are 6.5 mm diameter by 15.2 mm long. The cavity is discussed in detail in Refs. 15 and 21. The maximum Q we obtained is 4×10^7. The cavity has been tuned over a 300-MHz range while maintaining $Q>10^7$. The cavity used for the experiments described here was fabricated from copper and electroplated with lead. The cavity frequency with the halves pushed together was typically 70–100 MHz higher than the atomic transition frequency. Tuning to the atomic resonance required a gap between the halves of ≈25 μm.

Coarse tuning of the cavity was accomplished with a 1/4-28 screw driven from outside the vacuum chamber with a rack and pinion arrangement. A piezoelectric translator (PZT, Polytec Optronics model P-178.20) was used to fine tune the cavity over a range of approximately 10 MHz at liquid-helium temperatures. As shown in Fig. 6, four $\frac{1}{16}$-in-diam Teflon rods between the cavity halves provide the spring necessary to push back against the tuning mechanism. The two cavity halves are aligned with sapphire alignment pins.

1. Radiation temperature in the cavity

The thermometer mounted on the cavity measures the temperature of the cavity walls, typically 2 K. The mean blackbody photon number at this temperature is 0.8. If leakage of external radiation into the cavity can be neglected, the temperature of the radiation field is the wall temperature. Leakage of radiation through the

atomic and laser beam holes is not of concern because these are far below cutoff. However, the coupling hole needs careful consideration. This hole is designed to couple power between the cavity and the waveguide to monitor the cavity frequency and Q. The length of the coupling hole in the cavity was convenient for testing purposes.[21] However, this length would have allowed room-temperature radiation propagating down the waveguide to enter the cavity via the coupling hole. Therefore this hole was extended for the experiments described in this paper. A small wire loop inserted into the coupling hole was then necessary for monitoring the cavity. To search for possible residual effects of room-temperature radiation, we compared the multiatom-cavity oscillations with and without the coupling loop inserted slightly into the coupling hole. The two data sets are indistinguishable. The multiatom data presented in this paper were taken with the coupling loop adjusted to yield a 1.6% decrease in the power reflected from the cavity on resonance.

2. *Stray electric and magnetic fields*

The $46p \rightarrow 46s$ transition frequency is known accurately from our studies of the spectroscopy of calcium Rydberg states:[18] $\omega_0/2\pi = 35.331\,92(2)$ GHz. However, because stray electric fields within the cavity can cause a Stark shift, it was important to tune the cavity to the transition frequency *in situ*. We accomplished this by measuring the cavity induced population transfer from the $46p$ to $46s$ states as the cavity frequency was swept through the atomic resonance by the PZT tuner. The optimal combination of statistics and linewidth was obtained with about 15 atoms excited in the cavity. A potential of approximately 50 mV was applied between the cavity halves to null a field presumed due to contact and thermal potentials. The observed linewidth was typically 500 kHz, in agreement with calculations. The second-order Stark shift coefficient for the $46p(m=0) \rightarrow 46s$ transition is[22,23] 110 MHz/(V/cm)^2. The sign and magnitude of the observed shift of the atomic resonance frequency, typically a 60-kHz blue shift, were consistent with the assumption of a residual stray dc electric field of about 25 mV/cm. However, since our frequency resolution was about 60 kHz, this shift was too small to measure accurately.

A residual magnetic field can affect the experiment if it has a component perpendicular to the quantization axis, since this would cause precession among the m levels of the $46p$ state. To avoid this, the apparatus was constructed from nonmagnetic materials and the Dewar was surrounded by a single layer μ-metal shield. Based on our measurements with a gaussmeter, we estimate the residual magnetic field in the cavity to be 5–15 mG. This yields a maximum m-level splitting of 40 kHz, which is not significant.

The spectral width of the atom-cavity system decreases as the atom-cavity oscillation frequency decreases. Therefore the effects of stray electric and magnetic fields are most troublesome when the number of atoms is small.

B. Detector

The Rydberg atoms are observed with a two-channel field ionization detector that monitors the individual populations of the two states. After the atoms emerge from the cavity, they pass between two electric field plates whose separation decreases linearly. As a result, the atoms experience an increasing electric field. The ramp angle is chosen so that a single fixed voltage ionizes the two states above their respective channel electron multipliers (CEM's). The electrons released by the ionization pass through a slotted plate and are detected by one of the CEM's, which generates an electrical pulse for each ionized atom. If all the population is in one state, the background signal on the CEM for the other state is about 4% of the total signal. This small background signal is due primarily to the finite resolution of selective field ionization.

During the course of our cavity experiments, we discovered that our overall detection efficiency for the $46p$ atoms was typically 25%. Some of the loss of atoms can be attributed to the radiative decay of the atomic states: we estimate that approximately 60% of the $46p$ atoms and 40% of the $46s$ atoms reach the detector. This ratio agrees with our observations of the relative sizes of the cavity-induced transfer between the $46p$ and $46s$ states. We believe the remaining loss of approximately 50% is due to CEM inefficiency. Arnoldy *et al.*[24] have found that efficiency is lower for electrons which impinge on the CEM cone outside the diameter of or not parallel to the main body of the CEM. In view of these considerations, a 50% CEM efficiency in our system is plausible.

IV. OBSERVATION OF ATOM-CAVITY OSCILLATIONS

A. Collapse frequency $\nu_{\rm col}$ versus $\bar{N}_d$

By studying how $\nu_{\rm col}$ varies with $\bar{N}_d$, the general features of the system's behavior can be verified and the one remaining unknown parameter—the total detection efficiency ϵ_d—can be found. From Eq. (13) with $\bar{N} = \bar{N}_d/\epsilon_d$, we find

$$\nu_{\rm col} = \frac{a(\bar{N}_d/\epsilon_d)^{1/2}}{b + \ln(\bar{N}_d/\epsilon_d)} , \tag{19}$$

where the parameters a and b are determined from calculations of the time evolution of the system using the experimental values of Q and T. This is accomplished by the following procedure: The calculated time evolution curves are averaged using the experimentally determined distribution of N [Eqs. (17) and (18)], and then an averaged collapse frequency $\nu_{\rm col}(\bar{N})$ is extracted from this averaged time evolution curve for various values of $\bar{N}$. The parameters a and b are then obtained from a fit of $\nu_{\rm col}(\bar{N})$ versus $\bar{N}$ to Eq. (13). Finally, a fit of Eq. (19) to the measured $\nu_{\rm col}$ versus $\bar{N}_d$ with a and b fixed at these values yields the total detection efficiency ϵ_d.

Two representative sets of data from which $\nu_{\rm col}$ is extracted are shown in Fig. 7. To assist in extracting $\nu_{\rm col}$,

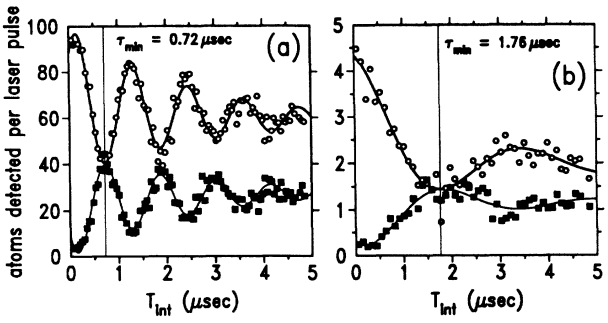

FIG. 7. Observed atom-cavity oscillations for $Q=1.18\times10^7$ and $T=2.17$ K for two values of $\bar{N}_d$. The solid curves are fits of the data to damped sinusoids, from which ν_{col} is extracted. The open circles are the atoms detected in the 46p state, and the closed squares are the atoms detected in the 46s state. T_{int} is the atom-cavity interaction time. The extracted values for ν_{col} in MHz are (a) 0.69(4) and (b) 0.28(4). (The numbers in parentheses denote the uncertainty in the last digit.)

we fit the data with the damped sinusoids shown. This procedure is repeated for various values of $\bar{N}_d$, yielding the values of ν_{col} versus $\bar{N}_d$ shown in Fig. 8. The solid curve in Fig. 8 is a fit of the data to Eq. (19) with a single adjustable parameter ϵ_d, which is found to be 0.24(1). The total detection efficiency was found to vary somewhat from day to day, ranging between 20% and 30%. The small but visible discrepancy between data and theory is discussed in Sec. V.

B. Observation of the system evolution

A series of time evolution curves for various values of $\bar{N}_d$ has been studied, using data from the set that was used to generate Fig. 8. Figures 9 and 10 display some of the data along with the calculated time evolution curves. Because the total detection efficiency has been previously determined (Fig. 8), there are no adjustable parameters. (However, the theoretical curves have been slightly rescaled for effects due to detector resolution and for the observed difference between the lifetimes of the 46p and 46s states.) The theoretical curves for Fig. 9 were obtained from the Bloch vector method, while those for Fig. 10 were calculated by the exact method. The agreement between theory and experiment for the larger numbers of atoms is satisfactory, but it is apparent that the data for $\bar{N}=15$ are only in crude agreement with theory.

We can also compare our results with theory for a sin-

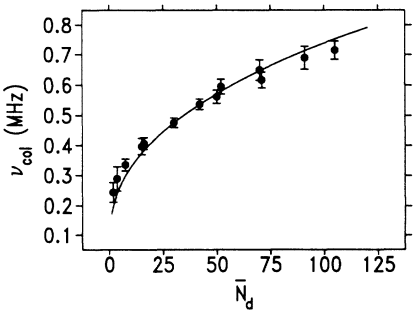

FIG. 8. Observed dependence of ν_{col} on $\bar{N}_d$ for $Q=1.18(5)\times10^7$, $T=2.17$ K, and $f_l=0.14$. The solid curve is a fit of the data to Eq. (19) which yields total detection efficiency $\epsilon_d=0.24(1)$. (The numbers in parentheses denote the uncertainty in the last digit.)

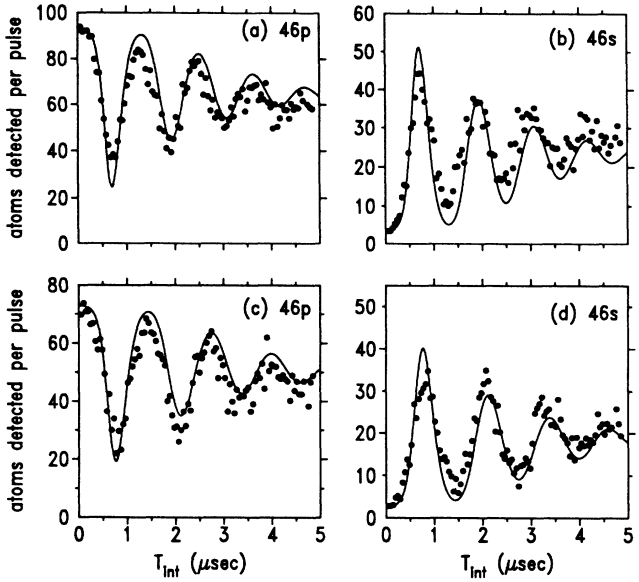

FIG. 9. Comparison of calculated and observed evolution of the system for large ensembles of atoms in the cavity. The calculations were performed using the Bloch vector model. Because ϵ_d has been determined previously (Fig. 8), there are no adjustable parameters. The closed circles are the number of atoms detected in the 46p and 46s states as a function of atom-cavity interaction time T_{int}. The amplitude of the theory curves are scaled to compare with data. (The theory curve for the 46s atoms has been multiplied by an additional factor of 0.7 to account for the shorter lifetime of the 46s state.) (a) and (b): $\bar{N}_d=93$, so the calculated mean number of atoms initially excited in the cavity using $\epsilon_d=0.24$ is $\bar{N}=380$. (c) and (d): $\bar{N}_d=73$, so $\bar{N}=300$.

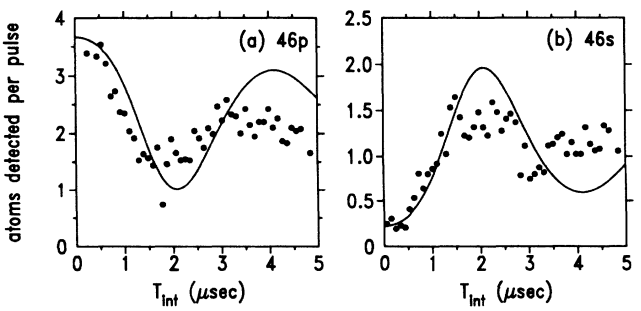

FIG. 10. Comparison of calculated and observed evolution of the system for a small ensemble of atoms in the cavity. The calculations were performed using the density-matrix method. (a) and (b): $\bar{N}_d=3.7$, so $\bar{N}=15$.

gle atom in the cavity. Single atom experiments are of special significance because they represent the limit of small systems. Furthermore, they have the experimental advantage of being free of much of the uncertainty in detection efficiency, assuming that the mean number of atoms detected per pulse is small compared to unity. For these studies we generally operated with an average of 0.04 atoms detected per laser pulse. Assuming a total detection efficiency of 20%, the probability of more than one atom excited in the cavity per laser pulse is only 1.8%. The observed and calculated evolution of a single atom in the cavity with $Q=1.5\times10^6$ and $T=1.95$ K are shown in Fig. 11. (A calculation for $T=9$ K is also shown for reasons discussed in the next section.) The relatively low value of Q in this particular run did not affect the observed behavior; other one-atom experiments with $Q\approx10^7$ yielded essentially the same results.

It is evident in Fig. 11 that the minor discrepancies pointed out in Figs. 8 and 10 have become major discrepancies in the single-atom experiments, effectively damping the resonance and destroying the oscillatory behavior.

V. POSSIBLE SOURCES OF THE DISCREPANCIES AT LOW N

Two effects could explain the discrepancies in our data at low numbers of atoms and the damping of single-atom oscillations: the radiation temperature could be higher than expected, and stray electric or magnetic fields could not be affecting the system. As discussed below, however, we cannot establish either of these effects alone as the cause of the problem.

A. Radiation temperature in the cavity

Blackbody radiation in the cavity would increase the atom-cavity oscillation frequency and cause the oscillations to wash out. Assuming a radiation temperature of 9 K yields a one-atom oscillation curve which has an initial collapse of the atomic population similar to the data (the thin theory curve in Fig. 11). Furthermore, the assumption of a radiation temperature of 9 K would also improve the agreement between data and theory for $\nu_{\rm col}$ versus $\bar{N}_d$, as shown in Fig. 12 (thick line). However, for large numbers of atoms, the effect of higher temperature is to increase $\nu_{\rm col}$ without changing the frequency of the subsequent oscillations. (The small number of blackbody photons becomes unimportant compared to the large number of photons released by the excited atoms.) Consequently, the assumption of a 9 K radiation temperature destroys the agreement shown in Fig. 9. Although experimental tests we have performed suggest that the temperature of the radiation field within the cavity is not substantially elevated above the temperature of the cavity walls, we have no independent measure of it.

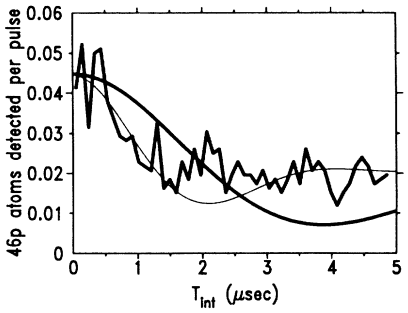

FIG. 11. Observation of the time evolution with a single atom in the cavity. The solid curves are calculations for $Q=1.5\times10^6$, $T=1.95$ K (thick line) and $T=9$ K (thin line). The total number of accumulated counts at $T_{\rm int}\approx0$ is 38.

B. Stray electric or magnetic field

Stray electric or magnetic fields can cause splitting of the m levels of the $46p$ state. For reasons discussed in Ref. 15, the stray magnetic field in our apparatus can be assumed to be perpendicular to the cavity axis. Therefore, if we choose the quantization axis along the stray magnetic field, only the $|m|=1$ states of the $46p$ level participate in the atom-cavity interaction. For this reason, the effect of a perpendicular magnetic field is to split the degeneracy of the upper level, yielding an effective three-level system. Furthermore, since the $m=\pm1$ states are degenerate in an electric field, any stray electric field not exactly parallel or perpendicular to the cavity axis also creates a three-level system. The effect of such splittings on the single-atom–cavity system is to speed up and damp the oscillations, which improves the agreement with the observed one-atom behavior (Fig. 11). The calculated oscillation frequency of the single-atom–cavity system in the presence of a source of m-level splitting is found to be given by[15]

$$\nu_{\rm osc}=(\nu_{\rm cav}^2+\nu_f^2)^{1/2}\ , \tag{20}$$

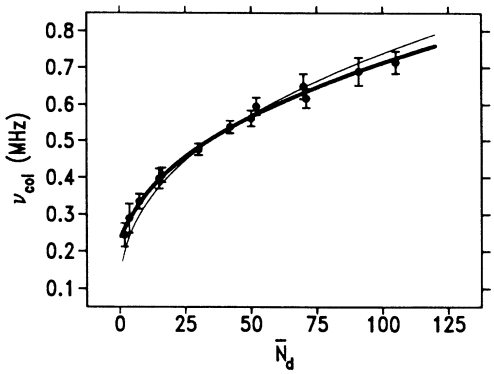

FIG. 12. Fits of $\nu_{\rm col}$ vs $\bar{N}_d$ to theory as discussed in Sec. V. The thick line is a fit of the data previously presented in Fig. 8 to theory assuming $T=9$ K which yields $\epsilon_d=0.39(1)$. This line is also a fit of the data to Eq. (21) with $T=2.17$ K yielding $\epsilon_d=0.29(1)$ and ν_f (m-level splitting) equal to 0.18(1) MHz. The circles are the data points and the thin line is the fit to Eq. (19) shown in Fig. 8, which assumes $\nu_f=0$ and $t=2.17$ K. (The numbers in parentheses denote the uncertainty in the last digit.)

where ν_{cav} is the oscillation frequency in the absence of the stray field and ν_f is the splitting between the magnetic sublevels induced by the electric or magnetic field. [The splitting of the $m=\pm 1$ sublevels in a magnetic field is 2.8 MHz/G. The splitting of the $|m|=1$ and the $m=0$ levels for the electric field case[22] is 39 MHz/(V/cm)^2.]

The interaction of an ensemble of nondegenerate three-level atomic systems with the radiation field in a cavity has not, to our knowledge, been analyzed in detail. If we make the ansatz that the multiatom oscillation frequency in a stray electric or magnetic field has the same form as Eq. (20), so that

$$\nu_{osc}(N)=[\nu_{col}^2(N)+\nu_f^2]^{1/2}\ , \tag{21}$$

where $\nu_{col}(N)$ is given by Eq. (13), we can fit our data to extract the magnitude of ν_f. Equation (21) is correct for $N=1$, and it has the proper limiting behavior for $\nu_{col}\gg\nu_f$. Figure 12 (thick line) shows the results of this fit to the data previously presented in Fig. 8. Note that the best fit of the data to Eq. (21) with a 2-K radiation temperature is identical to the fit based on calculations with $\nu_f=0$ and a 9-K radiation temperature. (However, the two approaches yield different values for the total detection efficiency.) The value extracted for the m-level splitting is $\nu_f=0.18(1)$ MHz, which seems unreasonably large. If it were due to an electric field at 45° to the cavity axis (the direction of maximum sensitivity), it would require a field of 70 mV/cm. Such a field would cause a shift in the transition frequency of 370 kHz, which was not observed. (The atomic resonance was shifted by at most 60 kHz for the data presented in Fig. 12.) If the splitting were due to a magnetic field, it would require a field of 65 mG. Because a magnetic field splits the transition without shifting it, it is difficult to diagnose a stray magnetic field given the large linewidth of the atomic response in the cavity. Our measurements of the residual magnetic field at the atomic beam with a gaussmeter indicate the field was only 5–15 mG, so a 65-mG magnetic field seems unlikely.

Although the assumptions of a 9-K radiation temperature or a stray electric or magnetic field in the cavity can account for some of the observed discrepancies between data and theory, for the reasons discussed above we do not believe that any one of these effects alone can reasonably provide the explanation. Possibly a combination of the three possibilities conspired to speed up and damp the atom-cavity oscillations for small numbers of atoms.

VI. CONCLUSIONS

We have achieved excellent time and state resolution in these experiments on atom-cavity interactions, allowing us to examine the dynamical behavior of the coupled atom-cavity system. Several aspects of the data were compared with theory, including the N dependence of the collapse frequency ν_{col} and the time evolution of the system. There is good agreement between theory and experiment for the data with more than about 50 atoms in the cavity. For lower values of N, a discrepancy between theory and experiment becomes evident. The discrepancy appears to be associated with a line broadening mechanism whose effects became progressively larger as N was decreased, until it reached the point that it effectively precluded useful single-atom studies. The most obvious sources of line broadening—temperature and stray electric or magnetic fields—do not appear to be able to individually account for the observations. Possibly a combination of these effects is the cause of the problem. In spite of the discrepancy between theory and experiment for small N, the data presented in this paper confirm our understanding of many aspects of the features of small ensembles of atoms interacting with a cavity in the quantum regime.

ACKNOWLEDGMENTS

We acknowledge a helpful discussion with J. M. Raimond. This work was supported by the Joint Services Electronics Program under Grant No. DAAL03-89-C-0001. Earlier research was supported by the U.S. Office of Naval Research (Grant No. N00014-79-C) and the National Science Foundation (Grant No. PHY84-11483).

*Present address: Science Research Laboratory, Inc., 15 Ward Street, Somerville, MA 02143.

†Present address: Kellogg Radiation Laboratory, California Institute of Technology, Pasadena, CA 91125.

[1]Serge Haroche and Daniel Kleppner, Phys. Today **42**(1), 24 (1989).

[2]Y. Kaluzny, P. Goy, M. Gross, J. M. Raimond, and S. Haroche, Phys. Rev. Lett. **51**, 1175 (1983).

[3]Gerald Gabrielse and Hans Dehmelt, Phys. Rev. Lett. **55**, 67 (1985).

[4]Randall G. Hulet, Eric S. Hilfer, and Daniel Kleppner, Phys. Rev. Lett. **55**, 2137 (1985).

[5]P. Goy, J. M. Raimond, M. Gross, and S. Haroche, Phys. Rev. Lett. **50**, 1903 (1983).

[6]D. Meschede, H. Walther, and G. Müller, Phys. Rev. Lett. **54**, 551 (1985).

[7]Gerhard Rempe, Herbert Walther, and Norbert Klein, Phys. Rev. Lett. **58**, 353 (1987).

[8]M. Brune, J. M. Raimond, P. Goy, L. Davidovich, and S. Haroche, Phys. Rev. Lett. **59**, 1899 (1987).

[9]Subir Sachdev, Phys. Rev. A **29**, 2627 (1984).

[10]S. Haroche, in *New Trends in Atomic Physics,* edited by G. Grynberg and R. Stora (North Holland, Amsterdam, 1984), p. 190.

[11]S. Haroche and J. M. Raimond, in *Advances in Atomic and Molecular Physics,* edited by D. R. Bates and B. Bederson (Academic, New York, 1985), Vol. 20, p. 347.

[12]H.-I. Yoo and J. H. Eberly, Phys. Rep. **118**, 239 (1985).

[13]E. T. Jaynes and F. W. Cummings, Proc. IEEE **51**, 89 (1963).

[14]R. H. Dicke, Phys. Rev. **93**, 99 (1954).

[15]Barbara J. Hughey, Ph.D. thesis, Massachusetts Institute of Technology, 1989.

[16]L. Moi, P. Goy, M. Gross, J. M. Raimond, C. Fabre, and S. Haroche, Phys. Rev. A **27**, 2043 (1983).
[17]Thomas R. Gentile, Barbara J. Hughey, Daniel Kleppner, and Theodore W. Ducas, Phys. Rev. A **40**, 5103 (1989).
[18]Thomas R. Gentile, Barbara J. Hughey, Daniel Kleppner, and Theodore W. Ducas, Phys. Rev. A (to be published).
[19]Thomas R. Gentile, Ph.D. thesis, Massachusetts Institute of Technology, 1989.
[20]J. Kirchgessner (private communication).
[21]Barbara J. Hughey, Thomas R. Gentile, Daniel Kleppner, and Theodore W. Ducas, Rev. Sci. Instrum. (to be published).
[22]This shift is calculated from second-order perturbation theory using our measured transition frequencies (Ref. 18) and computed matrix elements (Ref. 23).
[23]Myron L. Zimmerman, Michael G. Littman, Michael M. Kash, and Daniel Kleppner, Phys. Rev. A **20**, 2251 (1979).
[24]R. L. Arnoldy, P. O. Isaacson, D. F. Gats, and L. W. Choy, Rev. Sci. Instrum. **44**, 172 (1973).